ADVANCED ROBOTICS
https://doi.org/10.1080/01691864.2020.1857304

FULL PAPER

The influence of hip joint rotation of a physical assistant robot on curving motion

Yosuke Kuboki, Yasuhiro Akiyama, Shogo Okamoto and Yoji Yamada

Department of Mechanical Systems Engineering, Graduate School of Engineering, Nagoya University, Aichi, Japan

ABSTRACT
The use of physical assistant robots is expanding to activities of daily living. However, the risk of a user falling which can occur in various environments has not yet been considered despite this being a major concern for such robots. Therefore, this study focuses on curving motion, during which falling is more likely to occur, especially when the degree of freedom of the hip joint is restricted by the robot. We developed a physical assistant robot with an adjustable degree of freedom of hip rotation and observed the curving motions of the wearer under different joint restriction conditions. The result was statistically tested and the characteristics were extracted using factor analysis. It was noted that in the trials involving the restriction of hip rotation, the step length, pelvis yaw angle, and speed were significantly decreased with the decrease in hip rotation. However, as the participants changed their curving motion to compensate for the effect of joint restriction, the margin of stability varied slightly. This result suggested the necessity of implementing an assist algorithm that could change the gait motion to compensate and improve gait stability when curving.

ARTICLE HISTORY
Received 24 March 2020
Revised 23 September 2020
Accepted 18 November 2020

KEYWORDS
Physical assistant robot; hip rotation; curving gait; gait stability; factor analysis

1. Introduction

Recently, physical assistant robots have been developed to provide assistance in activities of daily living and industrial tasks [1,2]. However, the risk of falling is a critical hazard for individuals who use physical assistant robots for various applications, and thus should be carefully considered. When using a physical assistant robot, the ability to avoid falls likely decreases due to the restriction of motion caused by the mass of the robot [3,4], a mismatch of the joint mechanism [5], and/or a mismatch of the assist pattern [6]. Thus, to expand the applications of physical assistant robots, it is important to develop a method to analyze and decrease the risk of falling [7,8].

The complexity of the real life environment also makes it difficult to utilize physical assistant robots in daily life. Traditionally, physical assistant robots were used for gait rehabilitation on the treadmill [9,10]. While this use case is important and well-studied, the wearer is almost exclusively walking forward and motion in the sagittal plane dominates, which is not representative of a real-world environment. Thus, it is required to expand the motion ability of the physical assistant robot to fit various situations. Generally, it is required to add joints to expand the degree of freedom (DoF). However, additional joints potentially diminishes the assist torque because the assist torque is possibly absorbed as the motion and deformation of these joints especially when these joints can move freely and are not so rigid. Furthermore, it increases the size and mass of the robot, which makes the usability of the robot worse. Thus, the motion variability and assist performance may have the trade-off problem, which means that it is required to realize various motions using less DoF.

Human use various motions such as curving, sitting and standing, up and down stairs, and so on in the daily life. Among these motions, it is relatively easy to move in the sagittal plane because gait assist robots originally equipped the DoF along with this direction. However, in the daily living environment, people changes walking direction frequently [7,11–14]. The hip rotation and adduction/abduction, which is not critical for straight gait, are essential for curving motion [15,16]. One study on this topic demonstrated that if joint motion is restricted, the curving motion of a human wearing a physical assistant robot may be hindered [17]. However, although this study compared the wearer's motion with and without a robotic hip joint, the results did not apply to industrial applications of the robot as the hip joint was removed in the free condition. Furthermore, motion stability was not analyzed in that study. Thus, the effect

CONTACT Yasuhiro Akiyama akiyama-yasuhiro@mech.nagoya-u.ac.jp

Supplemental data for this article can be accessed here. https://doi.org/10.1080/01691864.2020.1857304

of joint restriction by a physical assistant robot on the curving motion and gait stability of the wearer should be further investigated.

In addition to hip flexion/extension, the internal/external rotation and adduction/abduction of the hip joint play a key role in performing curving motion [15,18]. In terms of gait motion, the internal/external rotation of the hip is the DoF that allows changes in the direction of the foot, and in turn the direction of the body, during curving motion. In contrast, adduction and abduction generate the motion of opening or closing the legs in the frontal plane. Therefore, even when walking in a straight line, these motions are used to place both feet close to the center of the body. In the case of curving, adduction and abduction of the hip are used to perform a lateral step, which causes an abrupt change in walking route [15]. Thus, internal/external rotation and adduction/abduction facilitate a smooth curving motion. Notably, implementation of internal/external rotation should be prioritized over adduction/abduction as turning the body is essential to curving motion.

In this study, the change in curving motion in response to restriction of hip rotation was investigated. A physical assistant robot frame, whose hip rotation joint could be fixed, was used to describe the relationship between joint restriction, curving motion, and gait stability by factor analysis.

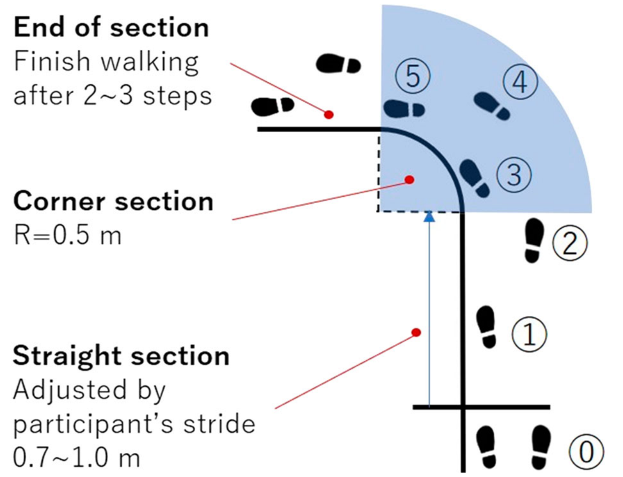

Figure 1. Curving path. The participants were instructed as to whether the left or right foot should be used for the first step. This figure shows the condition where the first step was with the left foot. The circled numbers denote the number of steps taken. The participants walked straight until the second step and performed a curving motion from the third step.

2. Experimental method

2.1. Apparatus

The participants walked along the path shown in Figure 1. The path consisted of a corner section with a radius of 0.5 m and two straight sections which were used for acceleration and deceleration. The motion of the participants in the corner section was recorded using a motion capture system (MAC 3D System, Motion Analysis Corporation, US). Thirty-five markers were attached to the body of each participant. The motion capture data were smoothed using a sixth-order Butterworth filter.

The frame of physical assistant robot, which was called MALO (motor actuated lower-limb orthosis), was attached to the user by the corset around the torso, belts around the thigh and shank, and shoes. In this experiment, actuators were not mounted on the robot in order to evaluate the effect of the DoF of a joint on curving motion, independent of stabilizing actuation. An overview of MALO is shown in Figure 2(a). MALO had hip, knee, and ankle joints, and all joints could rotate in the sagittal plane which is generally called flexion/extension. Moreover, the hip joint had an additional sliding mechanism to allow rotation in the horizontal plane by providing an additional DoF, as shown in Figure 2(b). This sliding mechanism could be fixed to restrict hip rotation. The range of motion of hip rotation was set to 30 degree, in accordance with previous work [15].

2.2. Participants

Eleven healthy, adult male subjects participated in this study. The participants had an average age of 22.4±2.4 years old (range: 18–25) and an average height and weight of 171.0±5.1 cm and 64.5±7.4 kg, respectively. The body mass index of the participants ranged between 18.5 and 25.2. The experiment was conducted with the approval of the Nagoya University ethics committee.

2.3. Protocol

Participants were outfitted in the experimental devices including well-fitting sportswear, motion capture markers, and MALO. Subsequently, participants continuously walked along the path shown in Figure 1. To control the gait timing to start curving at the appropriate position, the starting position was adjusted such that the curving motion started from the participant's third step. The participant was instructed to follow the path without stepping inside the curve.

The hip rotation was sequentially set as free and fixed (unrestricted and restricted) in each trial to observe the influence of joint restriction on curving motion. The subject are informed the restriction condition of trials and

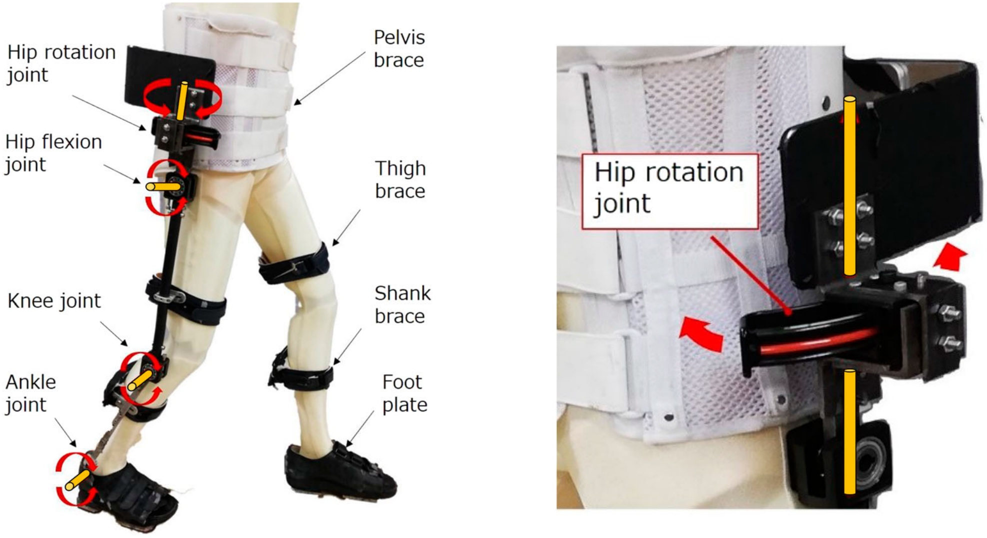

(a) (b)

Figure 2. The frame of physical assistant robot 'MALO'. The hip, knee, and ankle joints can rotate freely in the sagittal plane, which is called flexion/extension. The hip joint has an additional degree of freedom using the sliding mechanism, which allows to rotate in the horizontal plane. This sliding mechanism can be fixed to restrict hip rotation. (a) Overview. (b) Hip rotation joint.

get used to the device before start recording through several times of training trials. Furthermore, the leg used for the first step (left/right) was alternated between trials for each hip rotation condition. Both the left-foot-start and right-foot-start trials were recorded to evaluate the effect of gait timing on when an individual would start curving. Thus, each participant was tested under four conditions in total. Ten trials were recorded per condition for each participant, in random order.

3. Data processing

3.1. Parameter definition and calculation

Cycle time (CYtime) is the time between successive heel contacts (HCs) of the same foot. The timing of the HC is determined by measuring the minimum height of the heel marker. Step time (STtime) is the time between the successive HCs of different feet. The step length (STlength) is the distance between the heel markers of both feet at the time of HC in the sagittal plane. The direction of the sagittal plane is the direction perpendicular to the line consisting of the anterior superior iliac spine (ASIS) markers, which is determined with respect to the pelvis coordinate system. The center of mass (CoM) velocity (CoMV) is the velocity of the CoM at the time of HC; this parameter represents the gait speed. The motion of the CoM was calculated using Zatsiorsky's method [19] by fitting the positions of the markers to a human body model (SIMM, Musculographics Inc., US) [20].

The pelvis yaw angle (PAng) was introduced to evaluate the angle of the pelvis at each step in the horizontal plane. It is the change in the direction of the pelvis, which is determined from the rotation of the pelvis coordinate system in the global coordinate system between the HCs.

The longest (longest dist.) and shortest distances (shortest dist.) are the longest and shortest distances, respectively, between the center of curvature of the walking path and the CoM during the second to fifth steps.

The foot angle (FAng) is defined as the direction of the foot, which is determined from the line connecting the toe and heel markers in the pelvis coordinate system. The positive direction is towards the outside of the body. The hip rotation angle (HRAng) is defined as the rotation of the thigh with respect to the pelvis in the horizontal plane. The direction of the thigh is determined from the line of markers attached to the front and rear of the thigh. Since the timing of the HC does not match the timing of the maximum (external) and minimum (internal) HRAngs, the maximum and minimum values during a stride were used. The offsets of both parameters were adjusted using the data collected from an upright posture.

Hip flexion (TFlex) and extension (TExt) are calculated in the sagittal plane. The axis of the thigh is determined from the position of the greater trochanter, which is estimated from the positions of the ASIS and posterior superior iliac spine [21], and the knee marker. The hip angle is determined as the angle of the thigh axis projected on to the sagittal plane of the pelvis coordinate system. The offset is adjusted using the data collected

Table 1. Results of *t*-test: *p*-value, median value and quartile range of parameters.

	Left-foot-start			Right-foot-start		
	p-value	Unrestricted $n = 101$	Restricted $n = 107$	*p*-value	Unrestricted $n = 101$	Restricted $n = 103$
Cycle time						
CYtime:2–4 [s]		1.59; 1.50 – 2.22	1.58; 1.44 – 2.21		1.57; 1.47 – 1.88	1.55; 1.41 – 2.02
CYtime:3–5 [s]		1.60; 1.50 – 2.06	1.54; 1.43 – 1.89		1.54; 1.47 – 1.94	1.55; 1.39 – 2.05
Step time						
STtime:2-3 [s]		0.81; 0.75 – 1.08	0.82; 0.74 – 1.13		0.79; 0.72 – 1.03	0.78; 0.69 – 1.08
STtime:3-4 [s]		0.79; 0.73 – 1.09	0.79; 0.70 – 1.06		0.80; 0.71 – 0.92	0.78; 0.69 – 0.90
STtime:4-5 [s]		0.81; 0.74 – 0.97	0.75; 0.67 – 0.97		0.79; 0.71 – 1.03	0.78; 0.69 – 1.06
Step length						
STlength:2-3 [m]	**	0.46; 0.42 – 0.50	0.40; 0.35 – 0.44	**	0.52; 0.49 – 0.61	0.46; 0.42 – 0.55
STlength:3-4 [m]	**	0.43; 0.37 – 0.52	0.36; 0.30 – 0.44	**	0.82; 0.77 – 0.92	0.94; 0.87 – 1.03
STlength:4-5 [m]	**	0.44; 0.39 – 0.52	0.24; 0.19 – 0.31	**	0.46; 0.42 – 0.55	0.41; 0.37 – 0.44
CoM velocity						
CoMV2 [m/s]	**	0.66; 0.50 – 0.72	0.57; 0.39 – 0.69	**	0.63; 0.53 – 0.74	0.55; 0.45 – 0.66
CoMV3 [m/s]	**	0.57; 0.45 – 0.68	0.5; 0.37 – 0.61		0.62; 0.46 – 0.75	0.58; 0.40 – 0.70
CoMV4 [m/s]	**	0.58; 0.48 – 0.62	0.44; 0.33 – 0.56	**	0.59; 0.43 – 0.67	0.44; 0.34 – 0.55
CoMV5 [m/s]	**	0.55; 0.45 – 0.61	0.36; 0.27 – 0.46	**	0.51; 0.44 – 0.59	0.4; 0.33 – 0.50
Pelvis yaw angle						
PAng:2-3 [deg]		7.61; 5.42 – 11.38	8.54; 5.20 – 11.81	**	11.53; 5.13 – 17.23	3.86; 0.21 – 8.99
PAng:3-4 [deg]	**	26.66; 22.51 – 32.65	11.66; 8.84 – 16.76	**	27.77; 22.66 – 33.41	20.46; 17.26 – 26.00
PAng:4-5 [deg]	**	35.62; 30.55 – 40.15	25.56; 21.74 – 31.08	**	29.00; 25.35 – 33.48	19.8; 15.68 – 23.92
Distance						
Longest dist. [m]	**	0.84; 0.81 – 0.89	0.82; 0.80 – 0.85	**	0.88; 0.84 – 0.92	0.84; 0.80 – 0.89
Shortest dist. [m]	**	0.58; 0.57 – 0.60	0.6; 0.58 – 0.62		0.58; 0.57 – 0.61	0.6; 0.59 – 0.62
Foot angle						
FAng2 [deg]	*	7; 2.33 – 17.07	7.41; 3.72 – 17.37		−4.75; −8.72 – −1.48	−4.08; −6.08 – −1.17
FAng3 [deg]	**	0.84; −3.31 – 10.05	−0.98; −3.12 – 1.39	*	1.73; −7.88 – 7.17	0.80; −2.60 – 9.68
FAng4 [deg]	**	−1.48; −10.10 – 5.73	1.29; −4.76 – 7.88		4.78; −0.18 – 13.79	3.52; 1.00 – 6.55
FAng5 [deg]		1.93; −1.48 – 8.19	2.08; −1.02 – 4.03		3.02; −3.46 – 8.32	0.21; −3.93 – 7.12
Hip rotation angle						
HRAng:2–4 (Ext) [deg]	**	17.83; 14.17 – 25.41	13.42; 11.31 – 21.10	**	1.11; −1.11 – 5.48	0.33; −1.65 – 2.04
HRAng:2–4 (In) [deg]	**	2.28; −5.77 – 5.00	4.47; −2.62 – 6.19	**	−10.03; −12.96 – −7.24	−5.99; −10.52 – −3.80
HRAng:2–4 (Diff) [deg]	**	17.59; 14.18 – 19.94	9.86; 7.71 – 15.05	**	11.63; 8.43 – 15.45	5.76; 4.54 – 8.64
HRAng:3–5 (Ext) [deg]	**	1.78; −1.58 – 4.78	0.46; −3.59 – 1.73	**	19.97; 11.25 – 29.19	13.32; 10.99 – 21.99
HRAng:3–5 (In) [deg]	**	−11.96; −14.04 – −9.65	−5.40; −9.70 – −2.92	**	−0.37; −5.83 – 2.58	2.50; −2.87 – 5.98
HRAng:3–5 (Diff) [deg]	**	12.92; 9.90 – 16.96	5.01; 3.88 – 7.03	**	18.86; 15.24 – 25.53	10.75; 8.18 – 15.39
Thigh flexion/extension						
TFlex:2–4 [deg]		18.55; 9.29 – 30.63	19.84; 11.65 – 32.06		22.13; 11.63 – 34.30	20.19; 12.24 – 41.28
TExt:2–4 [deg]		−10.55; −19.72 – 1.71	−6.90; −13.43 – 3.97		−6.07; −15.19 – 2.39	−5.58; −15.56 – 2.24
TFlex-TExt:2–4 (Diff) [deg]		28.36; 25.42 – 30.76	26.31; 23.11 – 31.46		28.25; 25.16 – 34.24	28.18; 22.61 – 34.25
TFlex:3–5 [deg]		21.71; 11.93 – 34.37	19.24; 13.46 – 33.07		18.59; 8.29 – 35.20	18.38; 10.26 – 33.55
TExt:3–5 [deg]		−3.45; −15.15 – 7.28	−0.51; −11.5 – 6.31		−7.25; −16.42 – 6.97	−1.11; −11.32 – 8.27
TFlex-TExt:3–5 (Diff) [deg]		27.15; 20.40 – 31.61	26.46; 16.88 – 32.52	**	25.25; 22.87 – 30.02	22.45; 19.90 – 25.36
MoS traveling						
MoSt2 (Max) [m]		0.08; 0.06 – 0.13	0.09; 0.06 – 0.12		0.06; 0.00 – 0.1	0.08; 0.04 – 0.13
MoSt3 (Max) [m]	**	0.09; 0.06 – 0.12	0.11; 0.09 – 0.14		0.11; 0.10 – 0.14	0.13; 0.11 – 0.18
MoSt4 (Max) [m]		0.12; 0.10 – 0.14	0.12; 0.10 – 0.16		0.11; 0.07 – 0.14	0.11; 0.06 – 0.14
MoSt5 (Max) [m]	**	0.12; 0.09 – 0.15	0.09; 0.06 – 0.13		0.12; 0.10 – 0.15	0.14; 0.11 – 0.18
MoSt2 (Min) [m]	**	−0.20; −0.22 – −0.15	−0.17; −0.21 – −0.12		−0.19; −0.22 – −0.14	−0.17; −0.21 – −0.12
MoSt3 (Min) [m]	**	−0.22; −0.27 – −0.16	−0.17; −0.23 – −0.11	**	−0.26; −0.32 – −0.22	−0.22; −0.29 – −0.17
MoSt4 (Min) [m]	**	−0.21; −0.27 – −0.17	−0.13; −0.23 – −0.08	**	−0.17; −0.23 – −0.14	−0.10; −0.16 – −0.05
MoSt5 (Min) [m]	**	−0.22; −0.26 – −0.18	−0.06; −0.13 – −0.01	**	−0.23; −0.31 – −0.16	−0.17; −0.23 – −0.11
MoS mediolateral						
MoSl:2–4 (Max) [m]		0.21; 0.18 – 0.25	0.21; 0.19 – 0.24		0.19; 0.15 – 0.24	0.17; 0.14 – 0.22
MoSl:2–4 (Min) [m]		0.04; 0.03 – 0.06	0.05; 0.04 – 0.06		0.00; −0.04 – 0.01	−0.01; −0.04 – 0.02
MoSl:3–5 (Max) [m]	**	0.22; 0.16 – 0.27	0.15; 0.11 – 0.21		0.16; 0.13 – 0.19	0.15; 0.12 – 0.19
MoSl:3–5 (Min) [m]	**	0.00; −0.03 – 0.01	−0.01; −0.06 – 0.01		−0.03; −0.06 – 0.00	−0.03; −0.07 – −0.01

Note: $* \leq 0.05$, $** \leq 0.01$.

from an upright posture. In our analysis, the maximum flexion angle, maximum extension angle, and their difference were used. In Tables 1 and 2, this difference is expressed as 'TFlex-TExt (Diff)'.

The margin of stability (MoS), which is equivalent to the index of stability, is calculated independently in the traveling and mediolateral directions using the XCoM method [22]. XCoM is an index which consists of the position and velocity of the CoM to account for dynamic balance. The MoS is calculated as the distance between the XCoM and the base of support. A larger MoS indicates greater stability.

Table 2. Factor scores of curving motion.

	Left-foot-start: $n = 208$			Right-foot-start: $n = 204$		
	1st factor	2nd factor	3rd factor	1st factor	2nd factor	3rd factor
Contribution ratio [%]	23.2	14.0	13.4	20.2	16.5	12.4
Cycle time						
CYtime:2–4	0.92	0.34	0.16	0.92	0.34	0.11
CYtime:3–5	0.76	0.51	0.20	0.87	0.31	0.16
Step time						
STtime:4-5	0.93	0.24	0.16	0.91	0.30	0.11
Step length						
STlength:2-3	−0.23	0.53	−0.05	−0.22	0.48	0.68
STlength:3-4	−0.26	0.79	0.05	0.07	0.46	−0.49
STlength:4-5	−0.41	0.81	−0.02	−0.31	0.18	0.83
CoM velocity						
CoMV2	−0.83	0.24	0.01	−0.88	0.08	0.37
CoMV3	−0.91	0.12	0.01	−0.92	0.19	0.20
CoMV4	−0.87	0.33	−0.10	−0.76	0.04	0.59
CoMV5	−0.81	0.49	0.04	−0.82	0.10	0.38
Pelvis yaw angle						
PAng:2-3	−0.30	0.23	0.29	0.00	0.02	0.71
PAng:3-4	−0.17	0.73	−0.30	−0.56	0.35	0.44
PAng:4-5	−0.56	0.51	0.13	0.01	−0.14	0.53
Distance						
Longest dist.	−0.22	0.22	−0.19	0.47	0.03	0.35
Shortest dist.	0.12	−0.36	−0.31	0.05	−0.21	−0.14
Foot angle						
FAng2	0.19	0.47	0.08	0.35	0.22	0.03
FAng3	−0.05	−0.20	−0.94	0.02	−0.73	−0.06
FAng4	0.26	0.08	0.22	0.21	0.36	0.19
FAng5	0.07	−0.43	−0.76	−0.05	−0.56	0.25
Hip rotation angle						
HRAng:2–4 (Ext)	−0.22	0.31	−0.67	−0.26	0.14	0.07
HRAng:2–4 (In)	0.09	0.06	−0.80	−0.03	−0.14	−0.27
HRAng:2–4 (Diff)	−0.61	0.47	0.34	−0.21	0.27	0.34
HRAng:3–5 (Ext)	0.08	0.28	−0.02	−0.23	−0.26	0.50
HRAng:3–5 (In)	0.17	−0.41	−0.07	0.05	−0.44	0.26
HRAng:3–5 (Diff)	−0.10	0.65	0.06	−0.47	0.33	0.38
Thigh flexion/extension						
TFlex:2–4	0.10	0.07	0.58	−0.06	0.63	0.09
TExt:2–4	0.20	−0.02	0.46	0.17	0.36	−0.07
TFlex-TExt:2–4 (Diff)	−0.25	0.27	0.45	−0.33	0.66	0.25
TFlex:3–5	0.02	0.14	0.57	0.01	0.60	0.11
TExt:3–5	0.20	−0.18	0.36	0.09	0.47	0.04
TFlex-TExt:3–5 (Diff)	−0.27	0.51	0.43	−0.20	0.53	0.20
Margin of stability traveling						
MoSt2 (Max)	0.62	−0.07	0.42	−0.03	0.57	−0.19
MoSt3 (Max)	0.73	0.01	0.14	−0.48	0.67	−0.09
MoSt4 (Max)	0.22	0.06	0.50	0.08	0.75	0.02
MoSt5 (Max)	0.42	0.48	0.33	−0.36	0.70	0.40
MoSt2 (Min)	0.83	−0.22	−0.03	0.91	−0.18	−0.21
MoSt3 (Min)	0.79	−0.23	0.06	−0.22	0.40	−0.65
MoSt4 (Min)	0.51	−0.52	0.29	0.18	0.33	−0.59
MoSt5 (Min)	0.57	−0.27	0.28	−0.02	0.76	−0.34
Margin of stability mediolateral						
MoSl:2–4 (Max)	0.08	0.06	−0.35	−0.05	−0.13	0.05
MoSl:2–4 (Min)	−0.13	−0.26	−0.11	0.52	0.01	−0.23
MoSl:3–5 (Max)	−0.10	0.01	−0.58	0.29	0.08	0.16
MoSl:3–5 (Min)	0.32	−0.07	−0.13	0.55	−0.16	−0.01

The MoS in the traveling direction (MoSt) attains its minimum value shortly before HC and reaches its maximum soon after the whole foot touches the ground. These values are the minimum and maximum MoS of each step, respectively. The timings of the maximum and minimum MoS in the mediolateral direction (MoSl) are determined for each stride.

3.2. Analysis method

In advance, logarithmic transformation was performed. Stride parameters were compared between groups of different hip rotation restriction condition using MANOVA (Multivariate analysis of variance) [23]. Then, each parameter was compared using t-test, respectively [24].

Subsequently, factor analysis was used for both the left-foot-start and right-foot-start trials to extract the features of the curving motion [25].

4. Results

The second to fifth steps of each trial were analyzed, as all participants performed these steps in a curving motion regardless of restriction condition. Trials in which motion capture markers were entirely obstructed from view were omitted. Thus, 6–10 trials were analyzed from the test conditions for each participant with a total of 101–107 trials analyzed for each condition. The number of trials of each condition are provided in Table 1. The trajectory of footsteps of representative trials of each condition are shown in Figure 3

4.1. Difference in parameters for different joint restriction conditions

The parameters for each condition are listed in Table 1. The numbers beside each parameter correspond to the step number defined in Figure 1. Parameters were statistically compared by MANOVA and t-test between different restriction conditions. According to the result of MANOVA, significant difference were seen in both Left and Right foot start conditions ($p < .01$) between the unrestricted and restricted conditions.

4.1.1. Left-foot-start

As shown in Figure 1, the second and fourth steps correspond to the right foot in this case. Thus, the third and fifth steps correspond to the left foot. In the restricted condition, the values of HRAng and TFlex/Ext suggested that hip rotation decreased significantly, unlike the flexion and extension of the hip joint. With regards to the gait timing, which was represented by CYtime, STtime, STlength, and CoMV, the speed and step length decreased significantly, while there was a non-significant decrease in step time. Furthermore, it was noted that a decrease in the PAng corresponded to the decrease in step length. The difference in the MoS depended on the direction and side of the leg. In the traveling direction, the MoS

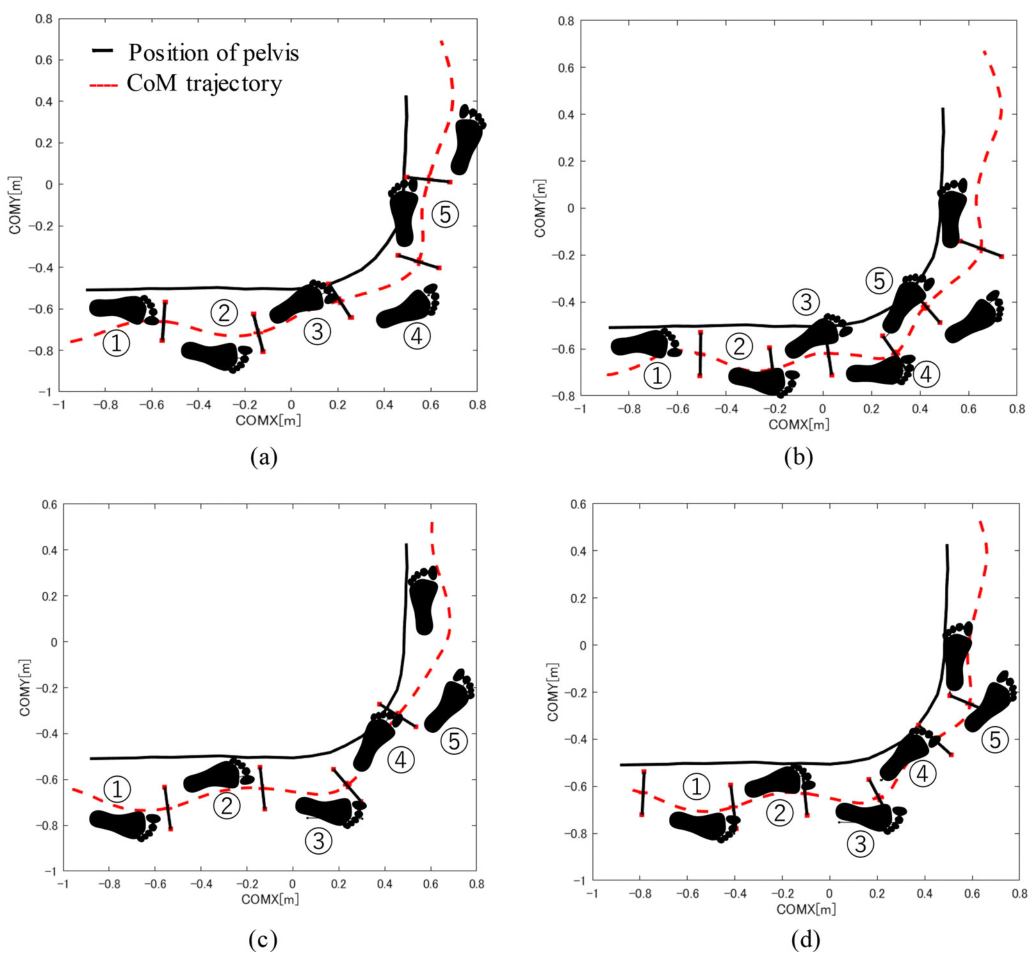

Figure 3. Position of footstep and CoM trajectory. Representative trials of each condition are displayed. The number placed beside each footstep stands for the step number. (a) Unrestricted, start from left step, (b) Restricted, start from left step, (c) Unrestricted, start from right step, (d) Restricted, start from right step.

of the left step was more affected by the restriction of the hip joint compared to the right step.

4.1.2. Right-foot-start

When the trial was started with the right foot, in contrast to the situation shown in Figure 1, the third and fifth steps corresponded to the right foot, and the second and fourth steps corresponded to the left foot. The trend in the hip angle and gait timing data was similar to the trend observed in the left-foot-start case. However, the difference between the MoS values was smaller in this condition.

4.2. Factor analysis

The results of the factor analysis are presented in Table 2. Three major factors were identified for each condition. To improve the accuracy of the analysis, the step time was consolidated as a single parameter.

4.2.1. Left-foot-start

The first factor was primarily related to the CYtime, STtime, CoMV, MoSt, and HRAng of the right stride (between the second and fourth steps). The parameters describing gait timing, except for STlength, were represented by this factor. The second factor primarily consisted of the STlength, PAng, and HRAng of the left stride (between the third and fifth steps). The third factor was represented by the FAng, HRAng of the right stride (HRAng:2–4), and TFlex/Ext. Notably, the second factor pertained to the parameters that significantly differed between the restriction conditions. Furthermore, HRAng was related to each of the three factors.

Subsequently, the relationship between the restriction condition and the factors was evaluated by performing the *t*-test. The results indicated that both the first and second factors differed significantly ($p < .01$) between the unrestricted and restricted conditions. In the restricted condition, the first factor became big whereas the second factor was small.

4.2.2. Right-foot-start

The first factor was related to the CYtime, CoMV, and MoSt, similar to in the left-foot-start case. However, the second factor consisted of the MoSt, FAng, and TFlex/Ext, which differs from the left-foot-start case. The third factor consisted of the STlength, PAng, and MoSt, and appeared to be similar to the second factor of the left-foot-start case, as it consisted of the parameters that significantly differed between the restriction conditions. The comparison of the factors between the different restriction conditions indicated that only the third factor was significantly reduced ($p < .01$) in the restricted condition.

5. Discussion

5.1. Curving motion under unrestricted condition

5.1.1. Left-foot-start

Although the participant entered the corner section from the third step (left step), the direction of the pelvis changed only slightly, according to the value of PAng:2-3 in Table 1. However, the slight internal rotation of the right hip (indicated by HRAng:2–4 (In)) suggested that the stepping leg was directed along the curve rather than the straight section.

At the fourth step, the participant started turning. To place the fourth step (right step) inside the curve, the stance leg rotated inward, as indicated by the rotation of the left hip (HRAng:3–5 (In)). Thus, PAng:3-4 increased at this step. Furthermore, the large PAng of the fifth step (PAng:4-5) suggested that the curving motion continued at the fifth step.

5.1.2. Right-foot-start

The participant started to curve from the third step (right step) in this case as well. The large internal rotation of the left hip (HRang:2–4 (In)) suggested that the third step was toward the inside of the curve, although PAng:2-3 was less than in successive steps. This motion resembled that of the fourth step in the left-foot-start case, and corresponded to the outside (right) leg.

Next, at the fourth step, PAng:3-4 increased, indicating the change in body direction had begun. At this step, the step length (STlength:3-4) was greater than that of the other steps. The long fourth step required the small external rotation of the left hip (HRang:2–4 (Ext)) to prevent to separate from the path.

5.2. Effect of the restriction of hip rotation

5.2.1. Left-foot-start

It appears obvious that the decrease in the HRAng is a consequence of joint restriction. Accordingly, the decrease in the PAng is likely caused by the decrease in hip rotation because hip rotation is essential to chang the direction of the pelvis. Furthermore, the CoMV and STlength decreased, which indicate a change in gait. The decrease in these parameters could be attributed to the fact that the participant walked with a short stride due to restriction of hip rotation.

According to the factor analysis, both the first and second factors were considerably affected by the restriction of the hip joint and included the HRAng. However, the parameters included in each factor were different. The first factor was related to the STtime, CoMV, MoSt, and HRAng:2–4(Diff)), which represents the stride of the outer leg. It is interesting to note that these parameters are not directly related to the curving motion. In contrast, the parameters of the second factor, such as the STlength and PAng, are parameters representative of curving motion. Furthermore, HRAng:3–5(Diff)), which denotes the stride of the inner leg, was included in this factor. Thus, according to the first factor, the restriction of the outer leg led to a slow gait, which corresponded to a decrease in speed and the STlength. In contrast, the second factor suggests that the restriction of the inner leg diminished the curving motion of each step, corresponding to a small PAng and STlength.

5.2.2. Right-foot-start

Although the trend of the parameters appears to be similar to that of the left start case, the effect of restriction seems to be smaller, especially for the MoS. In the factor analysis, the parameters of the first factor partly resembled those of the left start case, as the STtime and CoMV were related to this factor. However, the hip rotation was weakly related to this factor, and the effect of the joint restriction was not significant. The parameters related to the curving motion (i.e. STlength and PAng) were included in the third factor and the effect of the joint restriction was significant. Furthermore, the HRAng was also weakly related to this factor. Thus, in the right start case, the relationship between the restriction of a specific side and change in the motion is more obscure compared to that of the left start case.

5.3. Stability

According to the definition of the MoS, to improve the MoS, the step foot must be placed far from the CoM and the CoM height and velocity should be decreased [22]. However, none of the participants attempted to control their CoM height in this experiment. Thus, the change in the MoS was caused by changes in foot position and CoM velocity.

During the curving motion, the change in CoM velocity and step position was predominantly observed in the sagittal plane. Thus, the MoSl was slightly affected by restriction, especially in the right start case. Furthermore, the MoSl was not strongly related to the three major factors.

In the traveling direction, despite the joint restriction making it difficult for the participants to maintain balance naturally, the MoSt tended to increase in the restricted condition. It is possible that this arose from the participants compensating for the effect of joint restriction to maintain a balanced gait. Although the reduction of pelvis yaw angle in each step tended to decrease the MoS by decreasing the step length, the participants recovered from this effect by decreasing the gait speed. Furthermore, the MoSl was related to the CoMV rather than the STlength, as indicated by the first factors of both the left- and right-foot-start cases. It should be considered that MoS cannot currently be used as an absolute measure of stability because gait motion is fundamentally unstable. Thus, the value of the MoS is a relative index, and the qualitative difference in gait motion caused by compensation for joint restriction should be considered.

5.4. Limitations

For statistical analysis, the subjects with similar attribution, young male adults, were recruited in this experiment. However, the effect of joint restriction on the curving motion probably differs among various gait motions of different attribution of subjects. For example, it was reported that the elderly sometimes performes a different stepping strategy [26]. The experiment of subjects with various gait motions is required to generalize the result.

The curving motion maybe depends on the configuration of physical assistant robot because the mass, inertia, stiffness and other design parameters potentially affect gait motion [3,4,27]. In this study, the joint restriction was focused. Thus, the curving motion under the restriction of hip rotation were compared. Furthermore, common type of joint mechanism and fixation method are selected for generality. To evaluate the effect of configuration of assistant robot, another study, which compares the motion under different configurations, is required.

6. Conclusion

In this study, changes in gait and stability caused by a physical assistant robot were observed and analyzed during curving motion. Factor analysis was used to reveal important features of curving motion with and without joint restriction. The results suggested that restriction of hip rotation which is required for curving motion caused a significant decrease in the step length, speed, and pelvis yaw angle of each step. Furthermore, it was revealed that the participants changed their curving motion to compensate for the effects of joint restriction. However, considering gait stability, the MoS sometimes increased in the restricted condition. This trend can be ascribed to the fact that the participants maintained gait stability when compensating for joint restriction. The results of this study indicate that an assist algorithm for curving motion should be formulated for physical assistant robots. In particular, this algorithm should match the characteristics of curving motion, which differs according to the actuation mechanisms of different joints in the physical assistant robot. Therefore, the result of this study suggests the direction of the improvement of the joint structure and assist algorithm of the physical assistant robot, which will be used in the daily living environment.

Acknowledgments

We thank the support by JSPS KAKENHI Grant Number 17K01293 and the support of our group members, Yusuke Fukui and Takuma Igami. We also thank Ms. Xuan Yang.

Disclosure statement

No potential conflict of interest was reported by the author(s).

Funding

This work is support by JSPS KAKENHI Grant Number 17K01293.

Notes on contributors

Yosuke Kuboki received the B.E. and M.S. degree in engineering from Nagoya University, in 2018 and 2020, respectively. Since then, he has been working for HITACHI, Ltd. as an engineer. His research interests are human-robot interaction, wearable robotics, and safety engineering.

Yasuhiro Akiyama received the B.E. degree in engineering from Tokyo Institute of Technology, Tokyo, Japan, in 2006, and the M.S. and the Ph.D. degree in engineering from the University of Tokyo, Tokyo, Japan, in 2008 and 2011, respectively. Since 2016, he has been an assistant professor of Nagoya University, Japan. His main areas of research interests are mechanical safety, human–robot interaction, and manned space mission.

Shogo Okamoto received M.S. and Ph.D. degrees in information sciences in 2007 and 2010, respectively, from the Graduate School of Information Sciences, Tohoku University. Currently, he is an associate professor at the Department of Mechanical Systems Engineering, Nagoya University. His research interests include haptics, affective engineering, and human-assistive technology.

Yoji Yamada received a doctor degree from Tokyo Institute of Technology in 1990. In 2004, he moved from Toyota Technological Institute to National Institute of Advanced Industrial and Science Technology (AIST), as a group leader of Safety Intelligence Research Group in the Department of Intelligent Systems. In 2009, he moved to the Department of Mechanical Science and Engineering, Graduate School of Engineering, Nagoya Unversity as a professor. His current research interests include safety and intelligence technology in human–machine systems, and assistive robotics.

References

[1] Suzuki K, Mito G, Kawamoto H, et al. Intention-based walking support for paraplegia patients with robot suit hal. Adv Robot. 2007;21(12):1441–1469.
[2] Yasuhara K, Shimada K, Koyama T, et al. Walking assist device with stride management system. Honda R&D Tech Rev. 2009;21(2):54–62.
[3] Kodesh E, Kafri M, Dar G, et al. Walking speed, unilateral leg loading, and step symmetry in young adults. Gait Posture. 2012;35(1):66–69.
[4] Browning RC, Modica JR, Kram R, et al. The effects of adding mass to the legs on the energetics and biomechanics of walking. Med Sci Sports Exercise. 2007;39(3):515–525.
[5] Akiyama Y, Yamada Y, Ito K, et al. Test method for contact safety assessment of a wearable robot-analysis of load caused by a misalignment of the knee joint. In: 2012 IEEE RO-MAN: The 21st IEEE International Symposium on Robot and Human Interactive Communication. Paris, France: IEEE; 2012. p. 539–544.
[6] Akiyama Y, Higo I, Yamada Y, et al. Analysis of recovery motion of human to prevent fall in response to abnormality with a physical assistant robot. In: 2014 IEEE International Conference on Robotics and Biomimetics (ROBIO 2014). Bali, Indonesia: IEEE; 2014. p. 1493–1498.
[7] Lewis CL, Ferris DP. Invariant hip moment pattern while walking with a robotic hip exoskeleton. J Biomech. 2011;44(5):789–793.
[8] Akiyama Y, Kushida R, Yamada Y, et al. An analysis of recovery motion of a man wearing physical assistant robot in response to collision. In: 2015 IEEE International Conference on Systems, Man, and Cybernetics. Hong Kong, China: IEEE; 2015. p. 1089–1093.
[9] Beyl P, Van Damme M, Van Ham R, et al. Design and control of a lower limb exoskeleton for robot-assisted gait training. Appl Bionics Biomech. 2009;6(2):229–243.
[10] Veneman JF, Kruidhof R, Hekman EE, et al. Design and evaluation of the lopes exoskeleton robot for interactive gait rehabilitation. IEEE Trans Neural Syst Rehabil Eng. 2007;15(3):379–386.
[11] Lee ML, Dey AK. Embedded assessment of aging adults: a concept validation with stakeholders. In: 2010 4th International Conference on Pervasive Computing Technologies for Healthcare. Munchen, Germany: IEEE; 2010. p. 1–8.
[12] Zhou Z, Chen X, Chung YC, et al. Activity analysis, summarization, and visualization for indoor human activity monitoring. IEEE Trans Circuits Syst Video Tech. 2008;18(11):1489–1498.
[13] Glaister BC, Bernatz GC, Klute GK, et al. Video task analysis of turning during activities of daily living. Gait Posture. 2007;25(2):289–294.
[14] Chen B, Ma H, Qin LY, et al. Recent developments and challenges of lower extremity exoskeletons. J Orthop Translat. 2016;5:26–37.
[15] Akiyama Y, Toda H, Ogura T, et al. Classification and analysis of the natural corner curving motion of humans based on gait motion. Gait Posture. 2018;60:15–21.
[16] Akiyama Y, Okamoto S, Toda H, et al. Gait motion for naturally curving variously shaped corners. Adv Robot. 2018;32(2):77–88.

[17] Fukui Y, Akiyama Y, Yamada Y, et al. The change of gait motion when curving a corner owing to the motion restriction caused by a wearable device. In: 2017 IEEE International Conference on Systems, Man, and Cybernetics (SMC). Banff, Canada: IEEE; 2017. p. 525–530.
[18] Ounpuu S, Gage J, Davis R. Three-dimensional lower extremity joint kinetics in normal pediatric gait. J Pediatr Orthop. 1991;11(3):341–349.
[19] De Leva P. Adjustments to Zatsiorsky-Seluyanov's segment inertia parameters. J Biomech. 1996;29(9):1223–1230.
[20] Peter L, Scott D, Kenny S, et al. Software for interactive musculoskeletal modeling user guide 6.0. MusculoGraphics, Inc.; 2011.
[21] Bell AL, Pedersen DR, Brand RA. A comparison of the accuracy of several hip center location prediction methods. J Biomech. 1990;23(6):617–621.
[22] Bruijn S, Meijer O, Beek P, et al. Assessing the stability of human locomotion: a review of current measures. J R Soc Interface. 2013;10(83):20120999.
[23] O'Brien RG, Kaiser MK. Manova method for analyzing repeated measures designs: an extensive primer. Psychol Bull. 1985;97(2):316.
[24] Fay MP, Proschan MA. Wilcoxon-mann-whitney or t-test? On assumptions for hypothesis tests and multiple interpretations of decision rules. Stat Surv. 2010;4:1.
[25] Harman HH. Modern factor analysis. Chicago, IL: University of Chicago Press; 1976.
[26] Thigpen MT, Light KE, Creel GL, et al. Turning difficulty characteristics of adults aged 65 years or older. Phys Ther. 2000;80(12):1174–1187. doi:10.1093/ptj/80.12.1174. Available from: https://academic.oup.com/ptj/article-pdf/80/12/1174/31623454/ptj1174.pdf
[27] Arellano CJ, O'Connor DP, Layne C, et al. The independent effect of added mass on the stability of the sagittal plane leg kinematics during steady-state human walking. J Exp Biol. 2009;212(12):1965–1970.